Design and Implementation of the Discrete-Time Sliding Mode Controller for Trajectory Tracking of Quadrotor

Shun-Hung Tsai, Yi-Ping Chang, Ming-Li Chiang, Chao-Feng Tseng and Hung-Yi Lin*

***Abstract*—In this paper, we develop a robust position control of the quadrotor. The design of trajectory tracking controller for the quadrotor is divided into two parts, namely, attitude controller and position controller. First, the extrapolation method is utilized to transform the continuous-time dynamical model of quadrotor into discrete-time controller one. Then, a discrete-time sliding mode controller (DTSMC) is designed to ensure the position trajectory tracking capability in the presence of disturbance. Stability of the quadrotor is investigated by using Lyapunov stability analysis. Lastly, numerical simulations and experiments are demonstrated to show the validity and the feasibility of the proposed controller.**

***Index Terms*—Trajectory tracking, sliding mode control, quadrotor, Lyapunov stability.**

I. Introduction

NOWADAYS, unmanned aerial vehicle (UAV) has been used extensively for various areas, such as agriculture, fire-fighting, environmental protection and search and rescue applications. Among different types of UAVs, the quadrotor has many advantages. A quadrotor can take-off and land vertically in limited spaces and is easy to hover over the desired target. Moreover, an unmanned quadrotor is usually built by simple mechanical structure with the electrical actuators so it has better mobility in attitude changing and path planning than conventional helicopters. However, the quadrotor can be represented as a complex nonlinear system with coupled dynamics, and it is difficult to control accurately in terms of trajectory tracking. Thus, design of effective quadrotor controller is essential.

Classical linear control techniques have been utilized for trajectory tracking control of quadrotor in the literature. An optimal proportional-integral-derivative (PID) control based on integral of time multiplied by solution error indexes was developed in [1]. For the system error and data delay, the authors add Kalman filter to predict the change of error and get better trajectory estimation than that without a Kalman filter. A motion controller with nonlinear PID-type algorithm was designed in [2] to provide the robustness of tracking capability of the quadrotor when the disturbance is presented in one of the actuator. In [3], the position controller implemented with proportional-derivative (PD), PID and sliding mode control (SMC), respectively, for a V-tail quadrotor were compared. The simulation results show that the PD controller presents an error in the stable state that will not disappear as time goes on, and this can be a problem if an application with precision is required. The SMC has a facile and rapid response which drives the quadrotor converge to the desired point in the space.

Recently, model-based controller has shown that it has excellent performance in resolving nonlinear system control problem against uncertain model parameters and external disturbances. An observer-based dynamic sliding mode controller was introduced in [4]. The authors used a bank of nonlinear disturbance observers in conjunction with a matching set of generalized backstepping and sliding mode controllers to compensate the influence of the unmatched uncertainties to the system during the flight. Similarly, the SMC and backstepping methodology were combined to achieve position and yaw angle trajectory tracking. In the paper [5], Lyapunov theory was used in the stability analysis of the overall system.

Neural networks have also been studied for the trajectory tracking problem of quadrotor. A backstepping controller was designed by using radial basis function neural network in [6]. In [7], the authors use adaptive neural control technology to design a fixed-time backstepping controller. It ensures that the quadrotor tracks the desired trajectory well in finite time in spite of appearance of model uncertainties. A hierarchical controller was addressed to solve the path following problem in [8]. It consists of a model predictive controller (MPC) to track the reference trajectory together with a nonlinear $H\infty$ controller to stabilize the rotational movements.

The contribution of this paper is to implement the real-time trajectory tracking of quadrotor. The 10 degrees of freedom (DOF) inertial measurement unit (IMU) sensors, *i.e.*, 3-axis accelerometer, 3-axis magnetometer, 3-axis gyroscope and barometric pressure sensor, global positing system (GPS) and radio frequency (RF) sensors are integrated into quadrotor. In order to implement the flight controller with low computational complexity in the resource limited embedded system, the discrete-time sliding mode flight controller is designed [9, 10]. For signal processing, the Kalman filter is implemented into the resource limited embedded system. The rest of this paper is organized as follows: Section 2 illustrates the kinematics and dynamical model of the quadrotor. In Section 3, the design and stability analysis of the DTSMC for quadrotor are discussed. In Section 4, the data processing algorithms for the sensors

This paper is submitted on February 17th, 2021. This work was supported by the Ministry of Science and Technology of Taiwan, R.O.C., under Grant MOST-109-2221-E-027-078-, MOST- 109-2221-E-029-026, and MOST-108-3116-F-027-003-CC2.

Shun-Hung Tsai is with the Department of Electrical Engineering, National Sun Yat-sen University, Kaohsiung 80424, Taiwan, and also with the Graduate Institute of Automation Technology, National Taipei University of Technology, Taipei 10608, Taiwan, (e-mail:shtsai@mail.nsysu.edu.tw, shtsai@ntut.edu.tw).

Yi-Ping Chang is with the Graduate Institute Automation Technology, National Taipei University of Technology, Taipei 10608, Taiwan (e-mail: shtsai@ntut.edu.tw).

Ming-Li Chiang is with the Department of Applied Mathematics, Tunghai University, Taichung 407224, Taiwan (e-mail: mingli@thu.edu.tw).

Chao-Feng Tseng is with the National Chung-Shan Institute of Science and Technology, Taoyuan 32546, Taiwan (e-mail: megryn2k@gmail.com).

*****Correspondence: Hung-Yi Lin is with the High-Tech Facility Research Center, National Taiwan University, Zhubei 30264, Taiwan (e-mail: hylin@ntu.edu.tw).

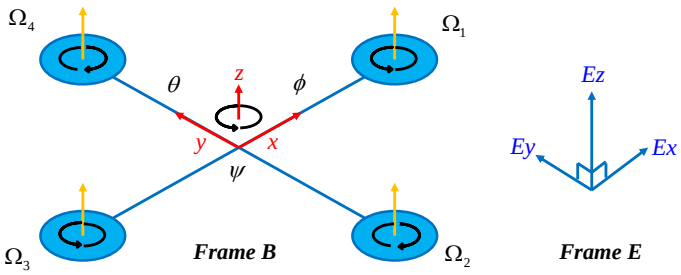

Fig. 1. The quadrotor frame system configuration.

equipped on the quadrotor is introduced. The flow chart of the trajectory tracking of the quadrotor is also presented. Section 5 demonstrates the simulations and experimental results of the developed quadrotor. The conclusions are given in Section 6.

II. Model Of The Quadrotor

A. Kinematics

The structure of the quadrotor is shown in Fig. 1. The quadrotor is actuated by the lift forces from four rotors located at the endpoint of the cross-shaped frame. The attitude and position of the quadrotor is controlled by adjusting the rotational speed of four rotors. Rotor 2 with the rotational speed Ω_2 and rotor 4 with the rotational speed Ω_4 rotates clockwise, in the meanwhile, rotor 1 with the rotational speed Ω_1 and rotor 3 with the rotational speed Ω_3 rotates counter-clockwise. In order to build the mathematical model of the quadrotor, it is assumed that the quadrotor frame is a symmetric grid body; the center of mass is at the geometric center of the body. The flapping dynamics of the frame are ignored.

To describe the attitude and the position of the quadrotor, we introduce two right-handed coordinate frames. The inertial, north-east-down, earth-fixed reference frame denotes as ***E***, and body-fixed frame denotes as ***B***. The inertial frame is based on the earth with its origin coincides with the origin of the body-fixed frame before taking off. The frame ***B*** is fixed with the quadrotor and the origin of the frame ***B*** is on the center of mass of body. The position vector of the quadrotor with respect to in the inertial frame ***E*** is $P_E = \begin{bmatrix} x_E & y_E & z_E \end{bmatrix}^T$, The position vector of the quadrotor with respect to in the body frame ***B*** is $P_B = \begin{bmatrix} x_B & y_B & z_B \end{bmatrix}^T$. The attitude of the quadrotor is described by Euler angle. The angle vector of the quadrotor with respect to the inertial frame ***E*** is $\alpha = \begin{bmatrix} \phi & \theta & \psi \end{bmatrix}^T$, in which ϕ is roll angle, θ is pitch angle and ψ is yaw angle. Hence, the angular velocity of the quadrotor with respect to the inertial frame ***E*** is $\dot{\alpha} = \begin{bmatrix} \dot{\phi} & \dot{\theta} & \dot{\psi} \end{bmatrix}^T$. All attitude angles are limited between $(-\pi/2, \pi/2)$. To convert the coordinates between two frames, the rotation matrix R_t is expressed as,

$$R_t = \begin{bmatrix} \cos\psi\cos\theta & \cos\psi\sin\theta\sin\phi - \sin\psi\cos\phi & \cos\psi\sin\theta\cos\phi + \sin\psi\sin\phi \\ \sin\psi\cos\theta & \sin\psi\sin\theta\sin\phi + \cos\psi\cos\phi & \sin\psi\sin\theta\cos\phi - \cos\psi\sin\phi \\ -\sin\theta & \cos\theta\sin\phi & \cos\theta\cos\phi \end{bmatrix} \quad (1)$$

The angular velocities of the quadrotor which are measured relative to the frame ***B*** is defined as $v = \begin{bmatrix} p & q & r \end{bmatrix}^T$. The transformation matrix R_ε is introduced to convert angular velocities of the quadrotor in the frame ***E*** from that in the frame ***B*** and it is written as [11, 12],

$$v = \begin{bmatrix} p \\ q \\ r \end{bmatrix} = R_\varepsilon \cdot \omega_E = \begin{bmatrix} 1 & 0 & -\sin\theta \\ 0 & \cos\phi & \cos\theta\cdot\sin\phi \\ 0 & -\sin\phi & \cos\theta\cdot\cos\phi \end{bmatrix} \begin{bmatrix} \dot{\phi} \\ \dot{\theta} \\ \dot{\psi} \end{bmatrix} \quad (2)$$

Similarly, the transformation matrix R_ε^{-1} is introduced to convert from the frame ***B*** to the frame ***E*** can be described as,

$$\dot{\alpha} = \begin{bmatrix} \dot{\phi} \\ \dot{\theta} \\ \dot{\psi} \end{bmatrix} = R_\varepsilon^{-1} \cdot \omega_B = \begin{bmatrix} 1 & \sin\phi\cdot\tan\theta & \cos\phi\cdot\tan\theta \\ 0 & \cos\phi & -\sin\phi \\ 0 & \dfrac{\sin\phi}{\cos\theta} & \dfrac{\cos\phi}{\cos\theta} \end{bmatrix} \begin{bmatrix} p \\ q \\ r \end{bmatrix} \quad (3)$$

B. Dynamics

The quadrotor model is simplified as a rigid body with point mass with four rotors symmetrically distributed around the center of mass. From the Newton's translational motion equation and Euler's rotational motion equation, the rigid body dynamics of a quadrotor with respect to the body-fixed frame ***B*** can be expressed as the following differential equations [13]

$$\begin{bmatrix} \ddot{x} \\ \ddot{y} \\ \ddot{z} \end{bmatrix} = -g \begin{bmatrix} 0 \\ 0 \\ 1 \end{bmatrix} + \frac{U_1}{m} \begin{bmatrix} \sin\psi\cdot\sin\theta\cdot\cos\phi - \cos\psi\cdot\sin\phi \\ \sin\psi\cdot\sin\theta\cdot\cos\phi - \cos\psi\cdot\sin\phi \\ \cos\theta\cdot\cos\phi \end{bmatrix} - \frac{1}{m} \begin{bmatrix} K_1\dot{x} \\ K_2\dot{y} \\ K_3\dot{z} \end{bmatrix} \quad (4)$$

$$\begin{bmatrix} \ddot{\phi} \\ \ddot{\theta} \\ \ddot{\psi} \end{bmatrix} = \begin{bmatrix} (I_x - I_z)\cdot\dfrac{\dot{\theta}\dot{\psi}}{I_x} \\ (I_z - I_x)\cdot\dfrac{\dot{\phi}\dot{\psi}}{I_y} \\ (I_x - I_z)\cdot\dfrac{\dot{\phi}\dot{\theta}}{I_z} \end{bmatrix} - J_r \begin{bmatrix} \dfrac{-\dot{\theta}}{I_x} \\ \dfrac{\dot{\phi}}{I_y} \\ 0 \end{bmatrix} \Omega_r + \begin{bmatrix} \dfrac{U_2}{I_x} \\ \dfrac{U_3}{I_y} \\ \dfrac{U_4}{I_z} \end{bmatrix} - \begin{bmatrix} \dfrac{K_4 l}{I_x}\dot{\phi} \\ \dfrac{K_5 l}{I_y}\dot{\theta} \\ \dfrac{K_6 l}{I_z}\dot{\psi} \end{bmatrix} \quad (5)$$

$$\begin{bmatrix} U_1 \\ U_2 \\ U_3 \\ U_4 \\ \Omega_r \end{bmatrix} = \begin{bmatrix} k\left(\Omega_1^2 + \Omega_2^2 + \Omega_3^2 + \Omega_4^2\right) \\ lk\left(-\Omega_2^2 + \Omega_4^2\right) \\ lk\left(-\Omega_1^2 + \Omega_3^2\right) \\ d\left(\Omega_2^2 + \Omega_4^2 - \Omega_1^2 - \Omega_3^2\right) \\ \Omega_1 - \Omega_2 + \Omega_3 - \Omega_4 \end{bmatrix} \quad (6)$$

Where m is the mass of the quadrotor, g is the acceleration of gravity and I_x, I_y and I_z are the moments components of inertial along the x-direction, y-direction and z-direction in the frame ***B***, respectively. $K_1 \sim K_6$ are drag coefficients and are positive constants. The term U_1 represents the total thrust on the

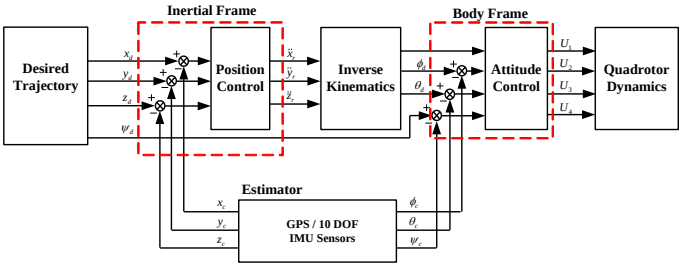

Fig. 2. Block diagram of the cotnrol system.

body in the *z*-axis. U_2 and U_3 denotes the roll and pitch inputs, respectively, U_4 presents a yawing moment. J_r is the rotor inertia, k represents thrust factor, d represents drag factor, l represents the length of each quadrotor's arm and Ω_r represents the overall speed of the rotor of the quadrotor.

III. Controller Design

In this section, the design of the DTSMC of the quadrotor will be presented in detail, and the stability analysis will also be discussed.

A. *Control Architecture*

The system structure of the quadrotor is shown in Fig. 2. A quadrotor is an underactuated force-controlled vehicle. Force actuation implies that translational and rotational commands are modeled as the second derivative of the position and attitude angle respectively. Due to the quadrotor's under actuation, only four DOFs out of its six DOFs $(x, y, z, \phi, \theta, \psi)$ can be selected as control input variables. Therefore, cascaded control architecture needs to be implemented between two loops, i.e., outer loop and inner loop, to resolve this problem. The inner loop is used for the attitude control. The outer loop is responsible for the position control of the quadrotor. The inputs of the position controller are the position error measurements on the *x*-, *y*- and *z*-axis, and their derivatives with respect to the inertial frame ***E*** obtained from the 10 DOF IMU sensors. The outer loop then calculates the associated control inputs $(\ddot{x}, \ddot{y}, \ddot{z})$ required in each axis. In this paper, three positional coordinates and the corresponding yaw angle (x, y, z, ψ) are chosen as the states to be tracked as shown in Fig. 2.

B. *Robust Trajectory Tracking Controller Design*

In order to design the discrete-time flight control of quadrotor, the continuous-time system of the quadrotor show in (4)-(5) is transformed into discrete-time system by using linear extrapolation method [9 -10]. The discrete-time dynamic model of the quadrotor is expressed as

$$\begin{bmatrix} x_{k+2} \\ y_{k+2} \\ z_{k+2} \end{bmatrix} = \begin{bmatrix} 2x_{k+1} - x_k + \Delta t^2 \left(\cos\phi_k \sin\theta_k \cos\psi_k + \sin\phi_k \sin\psi_k\right)\dfrac{U_{1,k}}{m} \\ 2y_{k+1} - y_k + \Delta t^2 \left(\cos\phi_k \sin\theta_k \sin\psi_k - \cos\phi_k \sin\psi_k\right)\dfrac{U_{1,k}}{m} \\ 2z_{k+1} - z_k + \Delta t^2 \left(\left(\cos\phi_k \cos\theta_k\right)\dfrac{U_{1,k}}{m} - g\right) \end{bmatrix} + \begin{bmatrix} \Delta t \dfrac{-K_1\left(x_{k+1} - x_k\right)}{m} \\ \Delta t \dfrac{-K_2\left(y_{k+1} - y_k\right)}{m} \\ \Delta t \dfrac{-K_3\left(z_{k+1} - z_k\right)}{m} \end{bmatrix} \quad (7)$$

$$\begin{bmatrix} \phi_{k+2} \\ \theta_{k+2} \\ \psi_{k+2} \end{bmatrix} = \begin{bmatrix} 2\phi_{k+1} - \phi_k + \left(\theta_{k+1} - \theta_k\right)\left(\psi_{k+1} - \psi_k\right)\dfrac{I_y - I_z}{I_x} + \Delta t^2 \dfrac{\mathrm{U}_{2,k}\, l}{I_x} \\ 2\theta_{k+1} - \theta_k + \left(\psi_{k+1} - \psi_k\right)\left(\phi_{k+1} - \phi_k\right)\dfrac{I_z - I_x}{I_y} + \Delta t^2 \dfrac{\mathrm{U}_{3,k}\, l}{I_y} \\ 2\psi_{k+1} - \psi_k + \left(\phi_{k+1} - \phi_k\right)\left(\theta_{k+1} - \theta_k\right)\dfrac{I_x - I_y}{I_x} + \Delta t^2 \dfrac{\mathrm{U}_{4,k}\, l}{I_z} \end{bmatrix} + \begin{bmatrix} \Delta t \dfrac{J_r\left(\theta_{k+1} - \theta_k\right)}{I_x}\Omega_r - \Delta t \dfrac{K_4 l\left(\phi_{k+1} - \phi_k\right)}{I_x} \\ \Delta t \dfrac{-J_r\left(\phi_{k+1} - \phi_k\right)}{I_y}\Omega_r - \Delta t \dfrac{K_5 l\left(\theta_{k+1} - \theta_k\right)}{I_y} \\ \Delta t \dfrac{-K_6\left(\psi_{k+1} - \psi_k\right)}{I_z} \end{bmatrix} \quad (8)$$

where Δt is the sampling time. To simplify the design of the trajectory controller, the kinematic and dynamic model of the quadrotor are divided into the actuated subsystem and the underactuated subsystem, respectively. The actuated subsystem involves the second order dynamic equations $\ddot{z}$ and $\ddot{\psi}$, while the underactuated subsystem involves the second order dynamic equations $\ddot{x}$ and $\ddot{\theta}$, $\ddot{y}$ and $\ddot{\phi}$, respectively. The goal of the actuated subsystem is to ensure that the states z_k and ψ_k will be converged to their desired equilibrium points z_k^d and ψ_k^d at the instant *k*, respectively. The objective of the underactuated subsystem is to ensure that the states (x_k, θ_k) and (y_k, ϕ_k) will be converged to their desired equilibrium points (x_k^d, θ_k^d) and (y_k^d, ϕ_k^d) at the instant *k*, respectively. As derived from [9, 10], the discrete-time sliding controller of the quadrotor can be described by the following differential equations.

$$U_{1,\mathrm{k}} = \frac{m}{\cos\phi_k \cos\theta_k}\left(\frac{-a_z dz_k + g + K_3 dz_k}{m} + \eta_1 s_{z,k}\right) \quad (9)$$

$$U_{2,\mathrm{k}} = \frac{I_x}{l a_3}\left(-a_1\left(\frac{g_{1,k}u_{1,k} - K_2 dy_k}{m}\right) - a_2 dy_k - a_3 f_{1,k} - a_4 d\phi_k + \eta_3 s_{\phi,k}\right) \quad (10)$$

$$U_{3,\mathrm{k}} = \frac{I_y}{l a_7}\left(-a_5\left(\frac{g_{2,k}u_{1,k} - K_1 dx_k}{m}\right) - a_6 dx_k - a_7 f_{2,k} - a_8 d\theta_k + \eta_4 s_{\theta,k}\right) \quad (11)$$

$$U_{4,\mathrm{k}} = I_z\left(\frac{-a_\psi d\psi_k + K_6 d\psi_k}{I_z} + \eta_2 s_{\psi,k}\right) \quad (12)$$

Where the coefficients in (9)-(12) can be chosen as follows:

$$\begin{bmatrix} a_1 \\ a_2 \\ a_3 \\ a_4 \\ a_5 \\ a_6 \\ a_7 \\ a_8 \end{bmatrix} = \begin{bmatrix} \dfrac{-12m}{(u_{1,k}\cdot\cos\psi_k)} \\ \dfrac{-8m}{(u_{1,k}\cdot\cos\psi_k)} \\ 1 \\ 6 \\ \dfrac{12m}{(u_{1,k}\cdot\cos\psi_k\cdot\cos\phi_k)} \\ \dfrac{8m}{(u_{1,k}\cdot\cos\psi_k\cdot\cos\phi_k)} \\ 1 \\ 6 \end{bmatrix} \tag{13}$$

$$\begin{bmatrix} dx_k \\ d\theta_k \\ dy_k \\ d\phi_k \end{bmatrix} = \begin{bmatrix} \dfrac{(x_{k+1}-x_k)}{\Delta t} \\ \dfrac{(\theta_{k+1}-\theta_k)}{\Delta t} \\ \dfrac{(y_{k+1}-y_k)}{\Delta t} \\ \dfrac{(\phi_{k+1}-\phi_k)}{\Delta t} \end{bmatrix} \tag{14}$$

$$\begin{bmatrix} g_{1,k} \\ g_{2,k} \\ f_{1,k} \\ f_{2,k} \end{bmatrix} = \begin{bmatrix} \dfrac{(\cos\phi_k \sin\theta_k \sin\psi_k - \sin\phi_k \cos\psi_k)}{m} \\ \dfrac{(\cos\phi_k \sin\theta_k \sin\psi_k + \sin\phi_k \cos\psi_k)}{m} \\ \dfrac{(d\theta_k d\psi_k (I_y - I_z) + J_r d\theta_k \omega_r - k_4 l d\phi_k)}{I_x} \\ \dfrac{(d\psi_k d\phi_k (I_z - I_x) - J_r d\phi_k \omega_r - k_5 l d\theta_k)}{I_y} \end{bmatrix} \tag{15}$$

where dx_k^d =0, dy_k^d =0, $d\theta_k^d$ =0, and $d\phi_k^d$ =0.

C. Stability Analysis

Proposition:

Consider the discrete-time system, the discrete equivalent of the system is given by (7) and (8), the design of DTSMC of quadrotor presented in (9)-(12) is asymptotical stability.

Proof:

The Lyapunov function candidates , $V_{j,k}$, is expressed as, [9,10]

$$V_{j,k} = \frac{1}{2} s_{j,k}^2 \tag{16}$$

Where $S_{j,k}$, is sliding surface at instant k, j are z, ψ, ϕ and θ, respectively. If the Lyapunov function shown in (16) meets the following condition as

$$\Delta V_{j,k} = s_{j,k+1}^2 - s_{j,k}^2 < 0, \qquad s_{j,k} \neq 0 \tag{17}$$

The discrete-time system will be asymptotical stability.

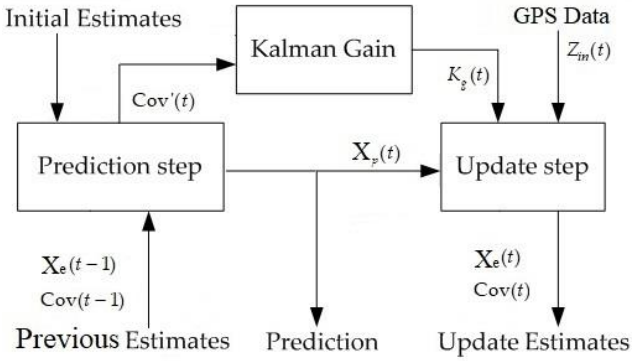

Fig. 3. Kalman filter recursive algorithm.

The analysis is givens as

$$\begin{aligned}\left(s_{j,k+1} - s_{j,k}\right)\cdot\operatorname{sgn}\left(s_{j,k}\right) &= \left(-\eta_i s_{j,k}\right)\Delta t\cdot\operatorname{sgn}\left(s_{j,k}\right) \\ &= -\eta_i \Delta t\left|s_{j,k}\right| < 0\end{aligned} \tag{18}$$

When the sampling time Δt is small and $(2-\eta-i)>0$, the following equation is derived as

$$\begin{aligned}\left(s_{j,k+1} + s_{j,k}\right)\cdot\operatorname{sgn}\left(s_{j,k}\right) &= \left[\left(2-\eta-i\right)s_{j,k}\right]\operatorname{sgn}\left(s_{j,k}\right) \\ &= \left(2-\eta-i\right)\left|s_{j,k}\right| > 0\end{aligned} \tag{19}$$

By multiplying (18) and (19), the (17) can therefore be concluded. Hence the DTSMC $U_{i,k}$ ($i=1,2,3,4$) shown in (9)-(12) satisfying (17) will guarantee that the discrete-time system will be asymptotically stable.

IV. Data Processing

In this section, the Kalman filter for GPS module and IMU sensor is discussed.

A. Kalman Filter Design

Kalman filter is an optimal recursive data processing algorithm to minimize the mean squared error between the actual data and estimated data. The computational advantage of the Kalman filter is that this algorithm uses only the current measured data and the previously calculated state and its error covariance matrix, no additional past information is needed. As shown in Fig. 3, there are two-step process in the Kalman filter, i.e., the prediction step and the update step [14].

In the prediction step, it predicts the current state variables.

$$X_p(t) = F\cdot X_e(t-1) \tag{20}$$

$$Cov'(t) = F\cdot Cov'(t-1)\cdot F^T + Q_{distb} \tag{21}$$

where F is state transient matrix, the current state variables $X_p(t)$ is derived from its previous estimate value $X_e(t-1)$ and F . $Cov'(t)$ is prior error covariance matrix and Q_{distb} is the expect value of the system disturbance. Kalman gain is counted for estimating the new predicted value and new uncertainty variance, the Kalman gain is defined as

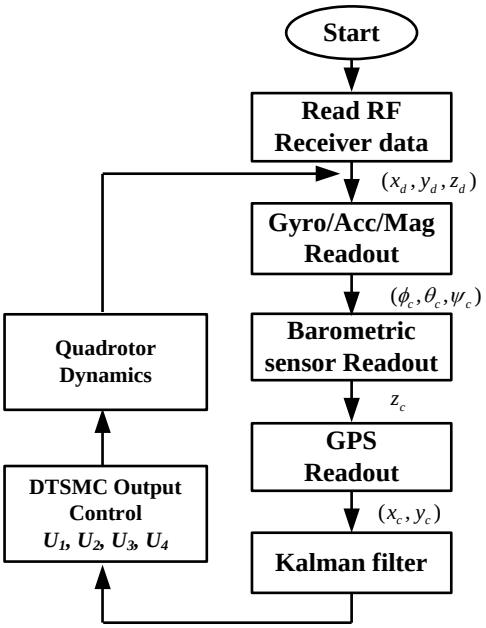

Fig. 4. The Flow chart of the trajectory tracking system.

$$K_g(t) = \frac{Cov'(t) \cdot H^T}{H \cdot Cov'(t) \cdot H^T + R_{error}} \tag{22}$$

where H is the noiseless transition matrix from the real state variables and R_{error} is the expect value of the error measurement.

In update step, the difference between predicted value and measured value which is obtained from the sensor readout is taken into consideration.

$$x_e(t) = x_p(t) + K_g(t)(Z_{in}(t) - H \cdot x_p(t)) \tag{23}$$

$$\mathrm{Cov}(t) = (I - K_g(t) \cdot H)\mathrm{Cov}'(t) \tag{24}$$

Where the update estimate $x_e(t)$ is derived from the measured data $Z_{in}(t)$. And $\mathrm{Cov}(t)$ is the error covariance of the estimate data.

B. *Flow Chart of Trajectory Tracking of Quadrotor*

Fig. 4 shows the flow chart of the trajectory tracking of quadrotor. The desired position is transmitted to the flight controller of the quadrotor via RF module. The current position data of the quadrotor is acquired by GPS and barometric pressure sensor. The current posture data of quadrotor is obtained by the gyroscope, accelerometer and magnetometer measured readouts. These data are processed by the Kalman filter and then act as the input parameters of the DTSMC, the tracking controller will calculate the shortest distance from the current position to the desired position. While the distance between the desired position and current position of the quadrotor is smaller than 1.5 *m*, the tracking controller will stop the tracking task, and the mission of trajectory tracking is finished.

V. Simulations and Experimental Results

In this section, the simulation and the experiments are illustrated to demonstrate the effectiveness of the developed DTSMC quadrotor. Subsection A shows the simulation results for trajectory tracking performance of the proposed quadrotor, and Subsection B demonstrates the experiments on dynamic real-time tracking capability of the quadrotor.

A. *Simulation Results*

The simulations are performed by MATLAB R2018b/Simulink. The computer consists of the Intel Core-i7-10700 CPU with 8GB of RAM and a 1T hard disk. For simplicity, the physical phenomenon present in the real world, such as the error range from the GPS module, and the friction of Brushless direct current (BLDC) motor are ignored. Table I lists the parameters of the quadrotor. Table II lists the parameter of our DTSMC.

TABLE I
Quadrotor Parameters

Variables	Value	Unit
m	2	kg
l	0.2	m
I_x=I_y	1.25	Ns^2/rad
I_z	2.5	Ns^2/rad
J_r	0.2	Ns^2/rad
K_i (i=1,2,3)	0.01	Ns/m
K_i (i=4,5,6)	0.012	Ns/m
g	9.8	m/s^2
b	5	Ns^2
	2	N/ms^2

TABLE II
DTSMC Parameters

Variables	Value	Variables	Value
a_z	1	a_ψ	1
η_z	2	η_ψ	2
a_1	$-12m/(u_{1,k}\cos\psi_k)$	a_5	$12m/(u_{1,k}\cos\phi_k\cos\psi_k)$
a_2	$-8m/(u_{1,k}\cos\psi_k)$	a_6	$8m/(u_{1,k}\cos\phi_k\cos\psi_k)$
a_3	1	a_7	1
a_4	6	a_8	6
η_3	5	η_4	5

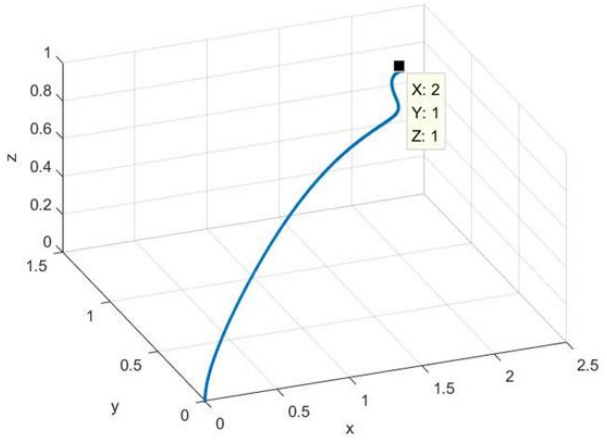

Fig. 5. The trajectory tracking of the quadrotor.

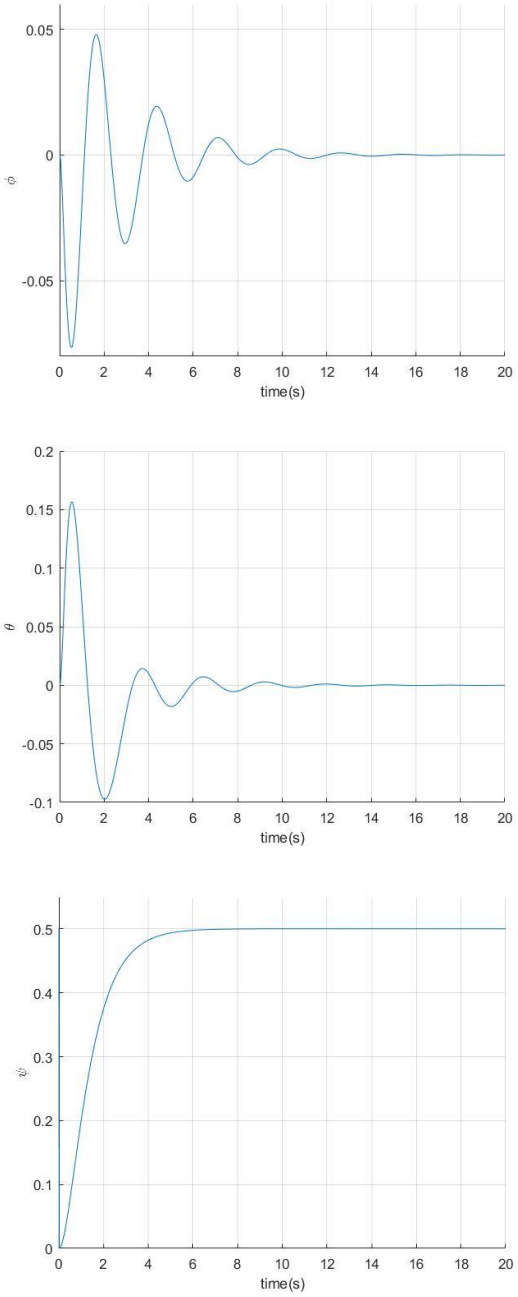

Fig. 6. Pitch, roll and yaw angles of the quadrotor.

Fig. 5 shows the trajectory tracking result of quadrotor. The initial position of body $P_c(0)=\begin{bmatrix}x_c & y_c & z_c\end{bmatrix}^T$ is set as $\begin{bmatrix}0 & 0 & 0\end{bmatrix}^T$, the initial Euler angle of the body $\alpha_c(0)$ is set as $\alpha_c(0)=\begin{bmatrix}\phi_c & \theta_c & \psi_c\end{bmatrix}^T=\begin{bmatrix}0 & 0 & 0\end{bmatrix}^T$ and the desired position of the body is set to $P_d(\mathrm{t})=\begin{bmatrix}2 & 1 & 1\end{bmatrix}^T$.

Fig. 6 shows the attitude tracking behavior of the quadrotor. It can be noted that the roll, pitch and yaw angles are converged to their desired value after 14 sec, 15 sec and 8 sec, respectively. Fig. 7 depicts the control input of the DTSMC of quadrotor. U_1, U_2, U_3 and U_4 are converged to their desired value after at 6 sec, 13 sec, 10 sec and 6 sec, respectively.

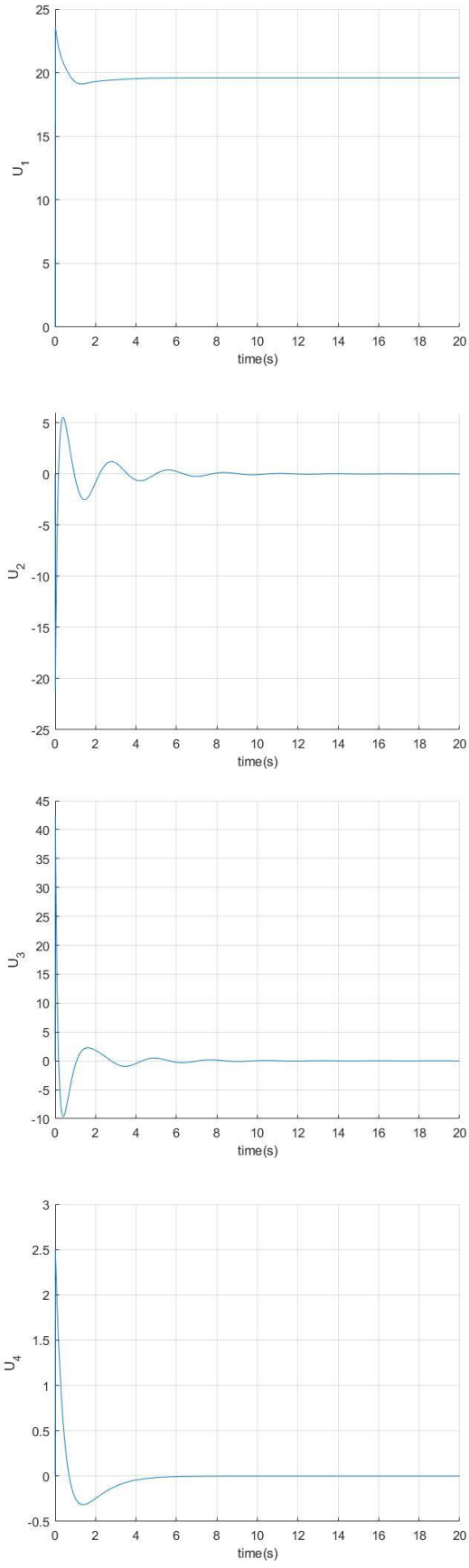

Fig. 7. Control input of the DTSMC of quadrotor.

Fig. 8. The quadrotor of experimental platform.

Fig. 9. The tracking plan of the experiment

(a)

(b)

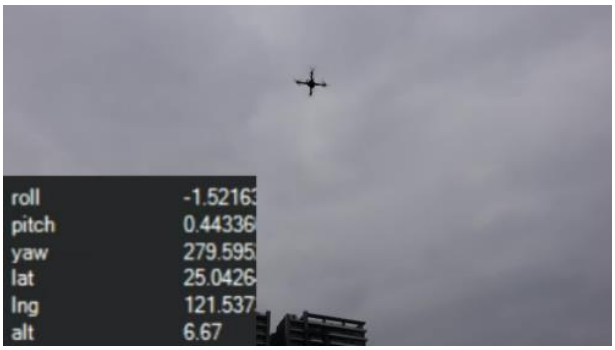

(c)

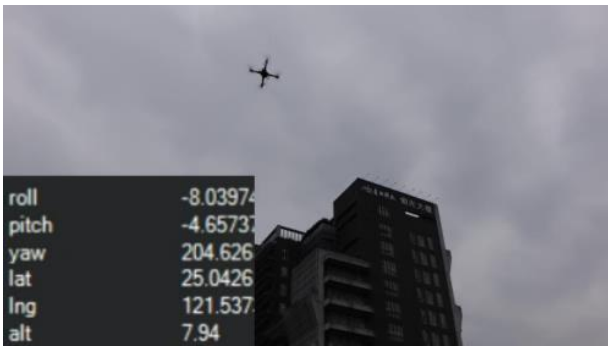

(d)

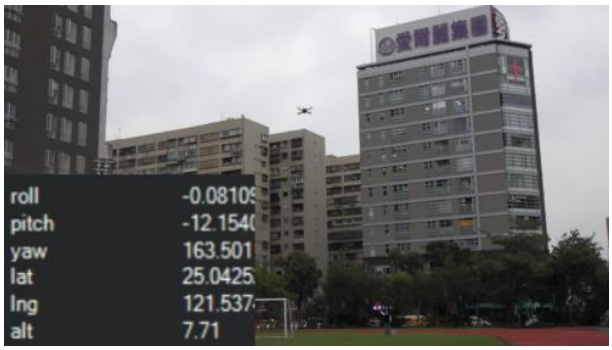

(e)

(f)

Fig. 10. The processes of the real-time trajectory tracking of quadrotor.

B. Experiments

The photo of the quadrotor is given in Fig. 8. In the proposed quadrotor, part number LSM303D is used for accelerometer and

(a)

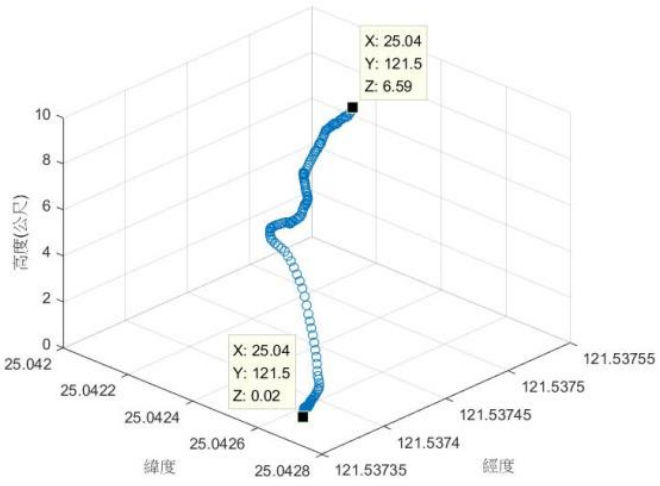

(b)

Fig. 11. The data log of the real trajectory path of the quadrotor.

magnetometer, part number L3GD20H is used for gyroscope, MS5611 is for barometric pressure sensor, NEO9-7M is for GPS module, 3DR Radio V2.0 is for RF module. Flight controller of the quadrotor is implemented by STM32F427 microcontroller.

Fig. 9 shows the trajectory tracking plan of our experiment. The experiment location is at stadium of the National Taipei University of Technology. The tracking plan is marked with the start point and the finish point on the google map. From Fig. 9, the start point is located at $(25^{\circ}02'33.5''\text{N}, 121^{\circ}32'14.5''\text{E})$, the final pint is located at $(25^{\circ}02'31.7''\text{N}, 121^{\circ}32'15.1''\text{E})$. In the experiment, the desired position of quadrotor is set at $(25.0420\text{N}, 121.537\text{E})$ and the flight height of the quadrotor is set to 7.1 *m*. Fig. 10(a)-(f) show the real-time trajectory tracking of the quadrotor. The red frame of Fig. 10(a) shows the real start position of the proposed quadrotor which is located at $(25.0416\text{N}, 121.537\text{E})$, the height of the quadrotor is 0.02 *m*, the red frame of Fig. 10(f) shows the real terminal position of the proposed quadrotor which is located at $(25.0421\text{N}, 121.537\text{E})$, the height of the quadrotor is 6.59 *m*.

The data log of the real trajectory path of the proposed quadrotor are shown in Fig. 11(a)-(b). Due to the physical phenomenon presented in the real world, i.e., the error range from the GPS module which is mounted on the quadrotor, the trajectory comparisons of the real tracking and desired ones are ignored and the simulation of trajectory tracking of the DTSMC of quadrotor is provided in Fig. 5.

VI. Conclusions

In this paper, a discrete-time sliding mode controller (DTSMC) is designed and implemented on the quadrotor. The kinematic and dynamic model of the quadrotor is discussed. Consider the stability problem of the DTSCM of the quadrotor, a Lyapunov function are utilized to prove that the DTSMC can achieve the asymptotically stable under some constraints. Lastly, simulations and experiments are provided to show the validity and the feasibility of the proposed controller.

For designing the next generation of the quadrotor, the shear effect of the quadrotor will be studied further to enhance the tracking performance of the quadrotor.

References

[1] F. Pan, L. Liu, and D. Xue, "Optimal PID controller design with Kalman filter for Qball-X4 quad-rotor unmanned aerial vehicle," *Trans. Inst. Meas. Control*, vol. 39, no. 12, pp. 1785-1797, July 2016.

[2] J. Moreno-Valenzuela, R. Pérez-Alcocer M. Guerrero-Medina, and A. Dzul, "Nonlinear PID-type controller for quadrotor trajectory tracking," *IEEE/ASME Trans. Mechatronics*, vol. 23, no. 5, pp. 2436-2447, Oct. 2018.

[3] J. J. Castillo-Zamora, K. A. Camarillo-Gomez, G. I. Perez-Soto, and J. Rodriguez-Resendiz, "Comparison of PD, PID and sliding-mode position controllers for V-Tail quadcopter stability," *IEEE Access*, vol. 6, pp. 38086-38096, July 2018.

[4] N. Fethalla, M. Saad, H. Michalska and J. Ghommam, "Robust observer-based dynamic sliding mode controller for a quadrotor UAV," *IEEE Access*, vol. 6, pp. 45846-45859, Sept. 2018.

[5] F. Chen, R. Jiang, K. Zhang, B. Jiang, and G Tao, "Robust backstepping sliding-mode control and observer-based fault estimation for a quadrotor UVA," *IEEE Trans. Ind. Electron.*, vol. 63, no. 9, pp. 5044-5056, Aug. 2016.

[6] M. A. Mohd Basri, A. R. Husain, and K. A. Danapalasingam, "Intelligent adaptive backstepping control for MIMO uncertain non-linear quadrotor helicopter system," *Trans. Inst. Meas. Control*, vol. 37, no. 3, pp. 345-361, June 2015.

[7] M. Wang, B. Chen and C. Lin, "Fixed-time backstepping control of quadrotor trajectory tracking based on neural network," *IEEE Access*, vol. 8, pp. 177092-177099, Sept. 2020.

[8] G. V. Raffo, M. G. Ortega, F. R. Rubio, "An integral predictive/nonlinear $H\infty$ control structure for a quadrotor helicopter," *Automatica*, vol. 46, pp. 29-39, 2010.

[9] S. Z. Sarpturk, Y. Istefanopulos and O. Kaynak, "On the stability of discrete-time sliding mode control," *IEEE Trans. Auto. Control*, vol. ac-32, no. 10, pp. 930-932, Oct. 1987.

[10] J.-J. Xiong and G. Zhang, "Discrete-time sliding mode control for quadrotor UAV," *Optik-International Journal for Light and Electron Optics*, vol. 127, issue 8, pp. 3718-3722, April 2016.

[11] J. Sun, Y. Wang, Y. Yu and C. Sun, "Nonlinear robust compensation method for trajectory tracking control of quadrotors," *IEEE Access*, vol. 7, pp. 26766-26776, March 2019.

[12] T. S. Alderete, "Simulator aero model implementation," [Online]. Available: https://robertheffley.com/docs/Sim_modeling/Alderete--NASA%20Ref%20Pub%201373.pdf

[13] E. Kayacan and R. Maslim, "Type-2 fuzzy loic trajectory tracking control of quadrotor VTOL aircraft with elliptic membership function," *IEEE/ASME Trans. Mechatronics*, vol. 22, no. 1, pp. 339-348, Feb. 2017.

[14] R. E. Kalman, "A New approach to linear filtering and prediction problem," *ASME J. Basic Eng.*, vol. 82, pp. 35-45, 1960.

[15] F. C. Park, B. Ravani, "Smooth invariant interpolation of rotations," *ACM Trans. Graph.*, vol. 16, pp. 277-295, 1997.

[16] S. O. H. Madgwick, A. J. L. Harrison and R. Vaidyanathan, "Estimation of IMU and MARG orientation using a gradient descent algorithm," *Proc.*

of the IEEE International conference on Rehabilitation Robotics, pp. 1-7, 2011.

[17] M. Admiraal, S. Wilson and R. Vaidyanathan, "Improved formulation of the IMU and MARG orientation gradient descent algorithm for motion tracking in human-machine interfaces," *Proc. of the IEEE International conference on Multisensor Fusion and Integration for Intelligent System (MFI 2017)*, pp. 403-410, 2017.

Shun-Hung Tsai received the B. S. degree from the Department of Industrial Education, National Taiwan Normal University, Taipei, Taiwan, in 1999, and the M. S. and Ph. D. degrees in 2001 and 2007, respectively, from National Cheng Kung University, Tainan, Taiwan, all in electrical engineering.

He was an Electrical Engineer in Philips Building Semiconductor from 2003 to 2005. From 2005 to 2006, he was a Control Engineer of China Steel Corporation. From 2006 to 2007, he served as a Process Integration Engineer in United Microelectronics Corporation. In 2008, he was an Associate Researcher with the Energy and Agile System Development, Metal Industrial Research and Develop Centre (MIRDC), Kaohsiung, Taiwan. Besides, he was an Assistant Professor in the department of electrical engineering, Chang Gung University of Taiwan in 2008. Furthermore, from 2009-2012, he was an Assistant Professor, an Associate Professor (2012–2018), and a Professor (2018–2021) in the Graduate Institute of Automation Technology, National Taipei University of Technology. He is currently a Professor of the Department of Electrical Engineering, National Sun Yat-sen University, Kaohsiung, Taiwan. Prof. Tsai received the Youth Automatic Control Engineering Award from Chinese Automatic Control Society in 2014, the Dr. Shechtman Young Researcher Award from National Taipei University of Technology in 2015. He has published over 120 journal and conference papers and book chapters on the research.

He has served as a program committee member and invited session chair for various international conferences and a reviewer for various international journals and international conferences. His major research interests include nonlinear control, intelligent control, system identification, pattern recognition, robotics and quadrotor.

Yi-Ping Chang received the B.S. degree and M.S. degree in Department of Earth Science from National Taiwan Normal University, Taipei, Taiwan, in 2000 and 2004, respectively. She is currently an earth science teacher in Taichung Second Senior High School, Taichung, Taiwan. Her current research interests and publications are in the area of the machine learning and pattern recognition.

Ming-Li Chiang received the Ph. D. degree in 2010 from Department of Electrical Engineering, National Taiwan University. From 2014 to 2016, he was a post doc researcher in University of Rome, La Sapienza. From 2017 to 2018, he joined the Center for Artificial Intelligence and Advanced Robotics in National Taiwan University. Since 2020, he served as an Assistant Professor in the Department of Applied Mathematics, Tunghai University. His research interests include nonlinear control system, switching systems, and multi-agent systems.

Chao-Feng Tseng received the B.S., M.S. and Ph.D. degree in electrical engineering from National Cheng Kung University, Tainan, Taiwan, in 2005, 2007 and 2016, respectively. He is currently an assistant researcher in National Chung-Shan Institute of Science & Technology. His current research interests and publications are in the area of the reconfigurable FPGA design and the image processing and compression.

Hung-Yi Lin received the B.S. degree in Department of Industrial Education from National Taiwan Normal University, Taipei, Taiwan, in 1999, the M.S. degree and Ph.D. degree in Department of Electrical Engineering from National Cheng Kung University, Tainan, Taiwan, in 2002 and 2012, respectively. He is currently a postdoctoral researcher in National Taiwan University. His current research interests and publications are in the area of the embedded system design and software and hardware co-design.